

Boundary layer eruption behind the bridge pillar model

K Strzelecka¹ and H Kudela¹

¹ Wrocław University of Technology, Faculty of Mechanical and Power Engineering,
Wybrzeże Wyspiańskiego 27, 50-370 Wrocław, Poland

E-mail: katarzyna.strzelecka@pwr.edu.pl

Abstract. Experimental quantitative (local velocity measurements by Laser Doppler Anemometry) and qualitative researches (visualization by dye marker) of flow around a bridge pillar model for the Reynolds number Re_D in the range of 40 up to 350 (for laminar, transitional and turbulent flow) were conducted. Re_D was the Reynolds number referred to the diameter of the model (cylinder), $D = 14,65$ mm.

1. Introduction

Experimental quantitative (local velocity measurements by Laser Doppler Anemometry) and qualitative researches (visualization by dye marker) of flow around a bridge pillar model for the Reynolds number Re_D of laminar, transitional and turbulent flow were conducted. Re_D was the Reynolds number referred to the diameter of the model $D = 14,65$ mm (vertical cylinder placed in shallow water).

It is known from the literature (e.g. [1]) that vortex structure above the plate can lead to the boundary layer eruption. It seems that similar phenomenon was observed behind a model of bridge pillar placed in shallow water. Previous investigations of flow past a vertical cylinder placed in shallow water were carried out for low values of h_w/D (h_w is the water depth in the test section), e.g. $h_w/D \ll 1$ [2] or $h_w/D = 0,5; 1; 2$ [3]. Chen and Jirka conducted extensive experimental researches for the case where the cylinder diameter D greatly exceeded the water depth. Akilli and Rockwell carried out investigations using a combination of visualization by dye marker and a PIV technique. They presented visualization results of vortex formation behind a cylinder for relatively low velocities in test section resulting in the Reynolds number (based on the water depth h_w): $Re_{hw} = U \cdot h_w / \nu$, where: U – mean velocity in a tunnel, ν – kinematic viscosity of water) from about $Re_{hwmin} = 500$ up to $Re_{hwmax} = 2500$.

Both authors mentioned above and also the others referred to the problem of flow past cylinder in shallow water (e.g. [4–6]) didn't investigate the vortex interaction with boundary layer and the boundary layer eruption. The phenomenon of nonstationary separation of a boundary layer leading to the eruption of fluid elements from the wall neighbourhood to the main flow was a subject matter of other researchers (e.g. [7–9]).

To put more light into the processes behind a model of bridge pillar for the Reynolds number Re_D of laminar, transitional and turbulent flow, authors of this paper decided to widen experiments on that subject.

2. Experimental setup

Experiments were conducted in water tunnel. Schematic of experimental setup working in closed circle is shown in Figure 1. In order to clean water in a system, part or whole mass of the water can be



exchanged. It is significant when carrying out visualization by dye marker researches, as colouring water can lead to gradual loss of contrast in recorded images.

Water is pumped from bottom reservoir (*BR*) by one, two or three pumps (P_1 , P_2 , P_3) – depending on the required flow rate, than it flows through the filter (*F*), rotameter (system is equipped with four rotameters of measuring ranges: R_1 : 2–19 l/h, R_2 : 18–180 l/h, R_3 : 170–1700 l/h, R_4 : 1500–15000 l/h), pressure vessel (*PV*) to damp pressure fluctuation (coming from pumps) and flow regulating valve (*FRV*) to inlet collector (*IC*). End of the pipe supplying the inlet collector is perforated and placed inside the collector to avoid excessive disturbances.

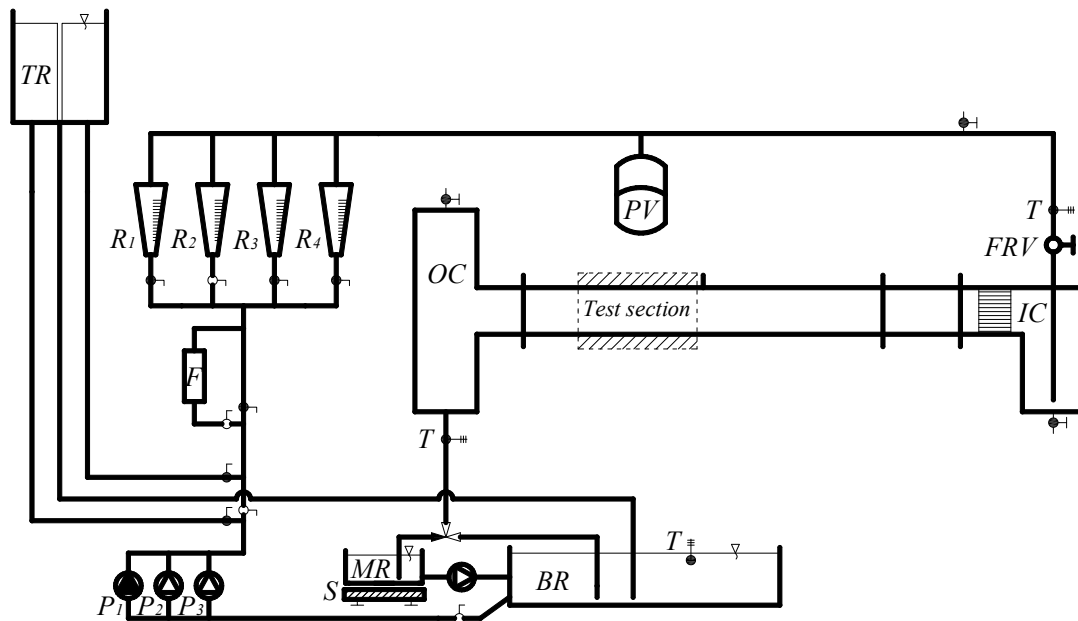


Figure 1. Schematic of experimental setup.

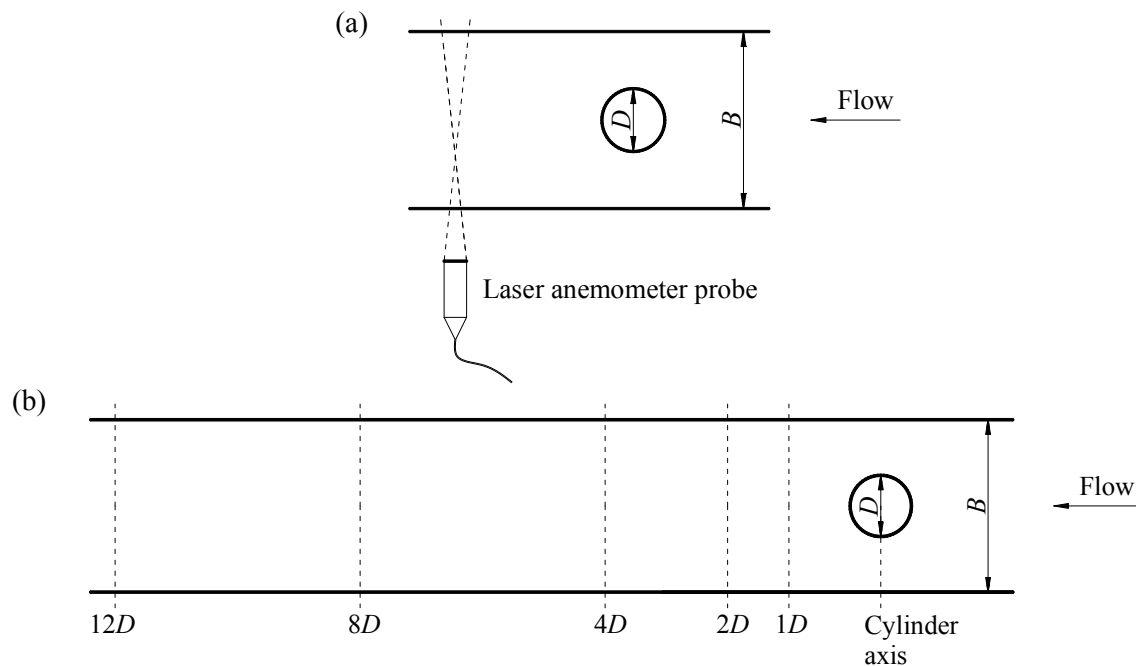
Rotameters fulfill the role of indicators. The accurate volumetric flow rate is done by mass measurement method. For low flow rates water is directed from the bottom reservoir (*BR*) to the top reservoir (*TR*), where the liquid level is fixed by overfall, than it flows through the rotameter (*R*) and flow regulating valve (*FRV*) to the inlet collector (*IC*). Next water inflows to the section consisting of two packets of drinking straws (5 mm in diameter) where disturbances are reduced. The length of each packet was determined in conformity with [10]. Then water flows through the Witoszynski nozzle behind which uniform velocity profile is formed. Next the liquid inflows to test section. The main test section built of plexi is $H = 100$ mm in depth, $B = 100$ mm in width and $L = 2000$ mm in length. Next water outflows to the outlet collector (*OC*), measuring reservoir (*MR*) placed on scales (*S*) – to determine the flow rate by mass method – and finally to bottom reservoir (*BR*). Temperature of the liquid is measured in three points: at inflow to the inlet collector (*IC*), at outflow from the outlet collector (*OC*) and in bottom reservoir (*BR*).

In order to determine the structure of flow in the area of the bridge pillar model (cylinder) impact, measurements of local averaged velocity (average in time) in the range of Reynolds numbers $Re_D \in \langle 40; 350 \rangle$ were conducted. Re_D values characterize flow in the tunnel with respect to the cylinder diameter D and, therefore laminar flow, laminar-turbulent transition as well as turbulent flow occur in test section [11]. Quantities characterising tested flows during anemometric researches are presented in Table 1. All the anemometric measurements were carried out for constant water depth in a tunnel $h_w = 65$ mm. Figure 2 shows schematic of test section for anemometric measurements.

Table 1. Fluid flow's hydrodynamic parameters for anemometric researches, water temp. $T = 22^\circ\text{C}$.

Re_D -	U mm/s	h_w mm	h_w/D -	q_v dm^3/h
40	2,61	65	4,44	61
100	6,53	65	4,44	153
150	9,79	65	4,44	229
250	16,32	65	4,44	382
350	22,84	65	4,44	535

Instantaneous local velocities were measured in 7 cross sections placed in a tunnel behind the bridge pillar model in the distances: $1D$, $2D$, $4D$, $8D$, $12D$, $16D$ and $20D$ (Figure 2(b)). The number of measuring points spaced across the width of the tunnel B was 39. Additionally, measurements of instantaneous local velocities in a cross section designated as "cylinder axis" were performed. In this case, measurements were made at 17 points placed between the tunnel wall and the cylinder wall. Laser Doppler Anemometry was the method applied for measuring local velocities (Figure 2(a)) in subsequent measuring points [12–14]. Data obtained from measurements (number of measurements $n = 500$ values of seeds particles velocity in each measuring point), were recorded in the form of text files and further processed. The obtained results enabled to determine the time-averaged local velocities (u), and then their profiles (relative values applied to mean velocity U , where $U = q_v/(h_w \cdot B)$) in the subsequent cross sections.

**Figure 2.** Schematic of test section for anemometric measurements: (a) plan view, (b) chosen cross sections in which researches were provided.

Vortex formation from a vertical cylinder in shallow water was investigated using visualization by dye marker. The vertical cylinder $D = 14,65$ mm in diameter was separated from the entrance to the test section and located at a distance of 1000 mm from it to ensure the fully formed velocity profile. Schematic of test section for visualisation experiments is shown in Figure 3. The dye injection was placed in the base of cylinder and carried out by means of the infusion pump.

Dye marker – through a tube ended with a needle – is placed inside the cylinder. The dye flows out from the cylinder at its bottom and is introduced into the boundary layer area (Figure 3 (c)). One

should be careful of the dye marker flow rate, not to have it very high and consequently not to disturb the formation of the vortex structure that is going to be observed behind the obstacle.

Visualization researches were carried out also for five values of the Reynolds number Re_D , but in contrast to anemometric measurements, they were extended to various water depth in the tunnel. Two visualisations were made for each Reynolds number as a consequent. In the first case the water depth was $h_w = 65$ mm, then it was reduced to $h_w = 30$ mm. The purpose of reducing the tunnel filling is to demonstrate the difference in the phenomena occurring in the flow around the cylinder without changing the Re_D , that is, assuming the diameter of the cylinder as a characteristic quantity. Flow characteristic values during visualization researches are summarized in Table 1.

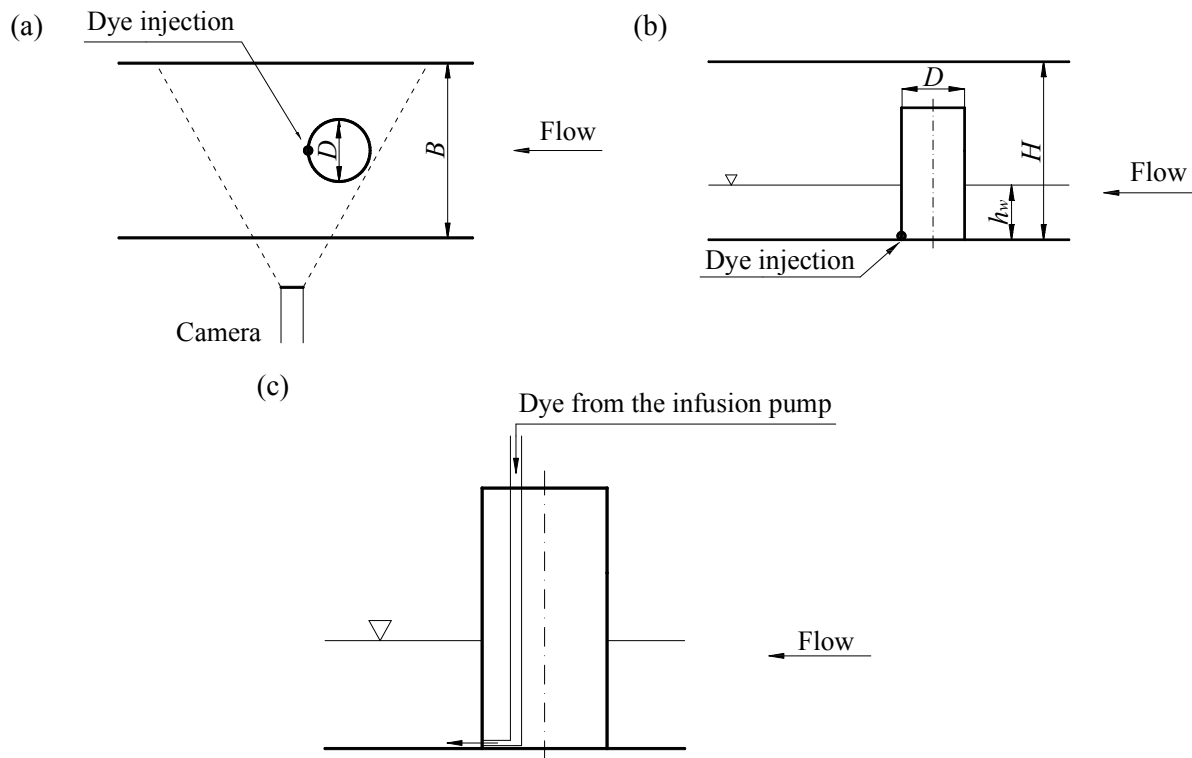


Figure 3. Schematic of test section for visualization experiments: (a) plan view, (b) side view, (c) dye marker letting in.

Table 2. Fluid flow's hydrodynamic parameters for visualisation researches, water temp. $T = 22^\circ\text{C}$.

Re_D -	U mm/s	h_w mm	h_w/D -	Re_{h_w} -	q_V dm^3/h
40	2,61	65	4,44	177	61
		30	2,05	82	28
100	6,53	65	4,44	444	153
		30	2,05	205	70
150	9,79	65	4,44	666	229
		30	2,05	307	106
250	16,32	65	4,44	1109	382
		30	2,05	512	176
350	22,84	65	4,44	1553	535
		30	2,05	717	247

3. Results of quantitative researches

Average local velocity measurements made by Laser Doppler Anemometry allowed to determine the velocity profiles in 7 cross sections behind the cylinder ($1D$, $2D$, $4D$, $8D$, $12D$, $16D$ i $20D$) as well as velocity distribution in the cross section signed as “cylinder axis” – at the distance from the wall of the tunnel to the cylinder wall. The analysis of quantitative measurements was carried out for five values of the Reynolds number Re_D : 40, 100, 150, 250 and 350. Figures 5, 7, 9, 11, 13 illustrate dimensionless velocity distribution obtained for examined Re_D in successive cross sections.

Average velocity distribution in the cross section signed as “cylinder axis” for subsequent Re_D are presented in Figures 4, 6, 8, 10, 12. It should be noted that in this cross section the dimensionless velocity distribution is the most disturbed for $Re_D = 40$, 100 and 150. For higher values of Re_D disturbances are noticeable only at the measuring points in the immediate vicinity of the tunnel wall and the wall of the cylinder.

For the Reynolds number of 40 (Figure 5), a recirculation zone was observed in the area of wake just behind the obstacle, in cross section $1D$ (Figure 5 (a)). This zone decreases with the distance from the obstacle and disappears in the distance of $8D$ behind the body flown around. In addition, in each of the cross sections till the distance of $16D$ the reverse flow zones near the tunnel walls were observed. In a distance $20D$ velocity profile is approximately formed.

For $Re_D = 100$ (Figure 7) significantly greater disturbances are visible than it was in the case of $Re_D = 40$. The recirculation zone in the wake of the cylinder has a slightly smaller width than that one observed for $Re_D = 40$, but here it reaches further – till the cross-section $2D$ (Figure 7 (a)–(b)). The reverse flow near the wall of the tunnel are observed till the distance of $8D$ (Figure 7 (a)–(d)). In the distance of $12D$ behind the cylinder disturbances of the velocity profile are still visible, velocity profile stabilizes at a distance of $16D$ and it looks similar in cross section $20D$.

Figure 9 shows the dimensionless velocity distribution for $Re_D = 150$. Both the shape of the dimensionless velocity profiles in successive measuring cross sections, and the range of the recirculation zones are here similar to those in the case of $Re_D = 100$.

For $Re_D = 250$ negative velocity values were measured in the area of the cylinder wake at a distance of $1D$, $2D$ and $4D$, thus the recirculation zone reaches further distance than it was for smaller values of the Reynolds number. There are no reverse flows observed near the walls of the tunnel. Velocity distribution looks very similar for the next examined Reynolds number, $Re_D = 350$. Here the recirculation zone is also observed only in the wake of the cylinder and reaches the cross-section $4D$. For both values of the Reynolds number the zone of reverse flows is much wider than for smaller values of Re_D . For $Re_D = 250$ and 350 velocity profile stabilizes at a distance of $12D$. In the cross sections $16D$ and $20D$ shapes of the velocity profiles are already very similar to each other.

The recirculation zone in the wake of the cylinder was observed for each examined Re_D Reynolds number. This zone is the more extensive the higher the Re_D is. That is connected with the regimes of flow around a cylinder, where laminar vortex street is observed for Re_D between 40 and 200, than transition to turbulence in the wake occurs for Re_D between 200 and 300 and finally the wake becomes completely turbulent for Re_D higher than 300 [11].

4. Results of qualitative researches

Qualitative researches performed with the use of visualization by dye maker were conducted for the same values of the Reynolds number Re_D as quantitative (LDA) measurement, but for two water levels ($h_w = 65$ mm, $h_w = 30$ mm) – in order to demonstrate the differences occurring in the flow with a Re_D Reynolds number (referred to the diameter D of the model) immutability.

Exemplary images of flow behind the bridge pillar model for subsequent Re_D and both water depths are presented in Figures 14–18.

For $Re_D = 40$ and $h_w = 65$ mm (Figure 14 (a)) the dye marker spreads along the bottom surface of the test section, in the area of the boundary layer. Then a thin thread of the dye marker is slowly displaced from the boundary layer area. This thread of dye is taken away and dissipated by the main stream of water flowing in a tunnel at a height about $1/3$ of the water depth.

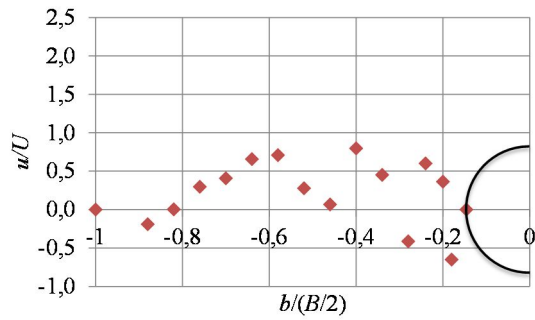


Figure 4. Average velocity distribution in the cross section of the cylinder axis for $Re_D = 40$

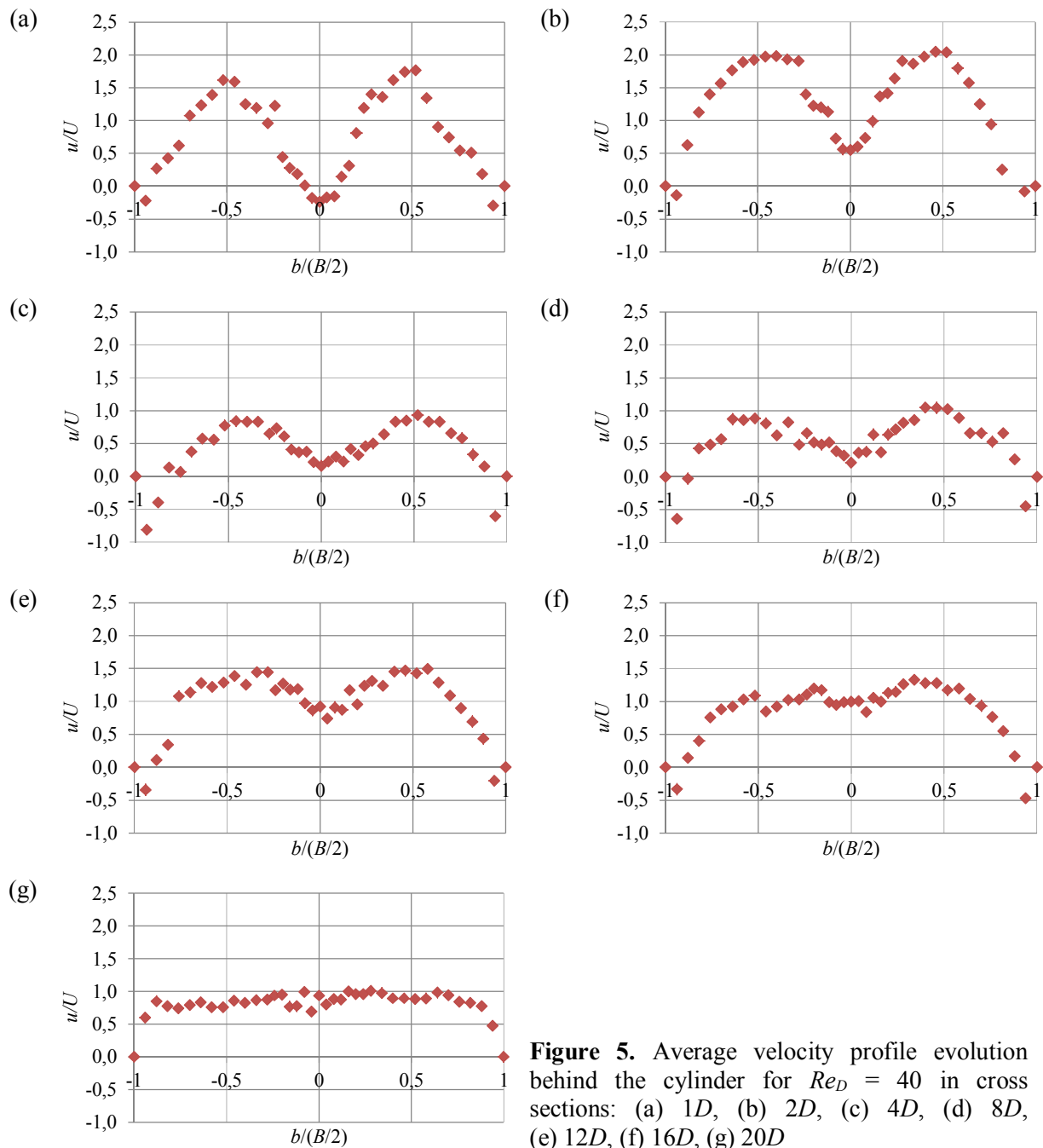


Figure 5. Average velocity profile evolution behind the cylinder for $Re_D = 40$ in cross sections: (a) $1D$, (b) $2D$, (c) $4D$, (d) $8D$, (e) $12D$, (f) $16D$, (g) $20D$

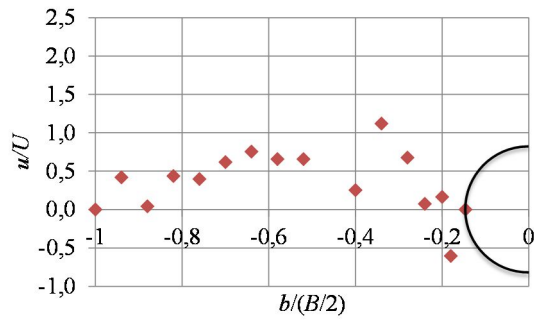


Figure 6. Average velocity distribution in the cross section of the cylinder axis for $Re_D = 100$

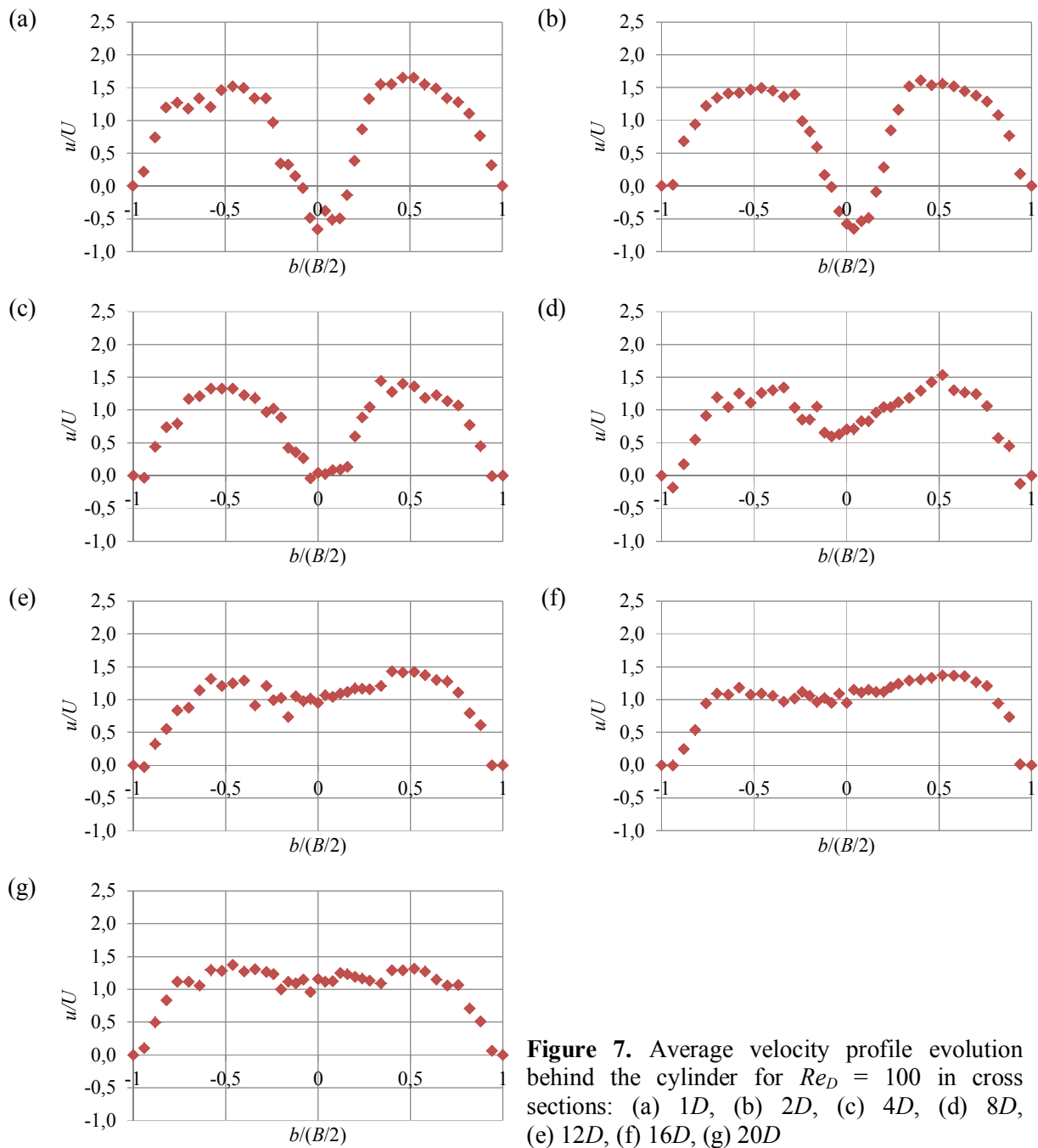


Figure 7. Average velocity profile evolution behind the cylinder for $Re_D = 100$ in cross sections: (a) $1D$, (b) $2D$, (c) $4D$, (d) $8D$, (e) $12D$, (f) $16D$, (g) $20D$

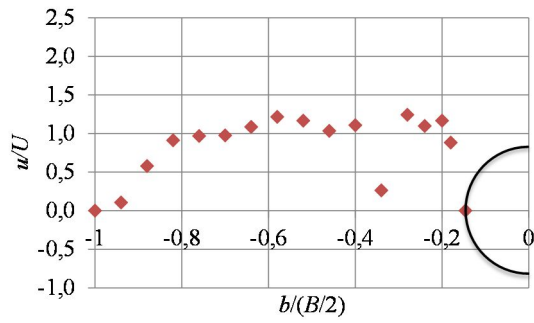


Figure 8. Average velocity distribution in the cross section of the cylinder axis for $Re_D = 150$

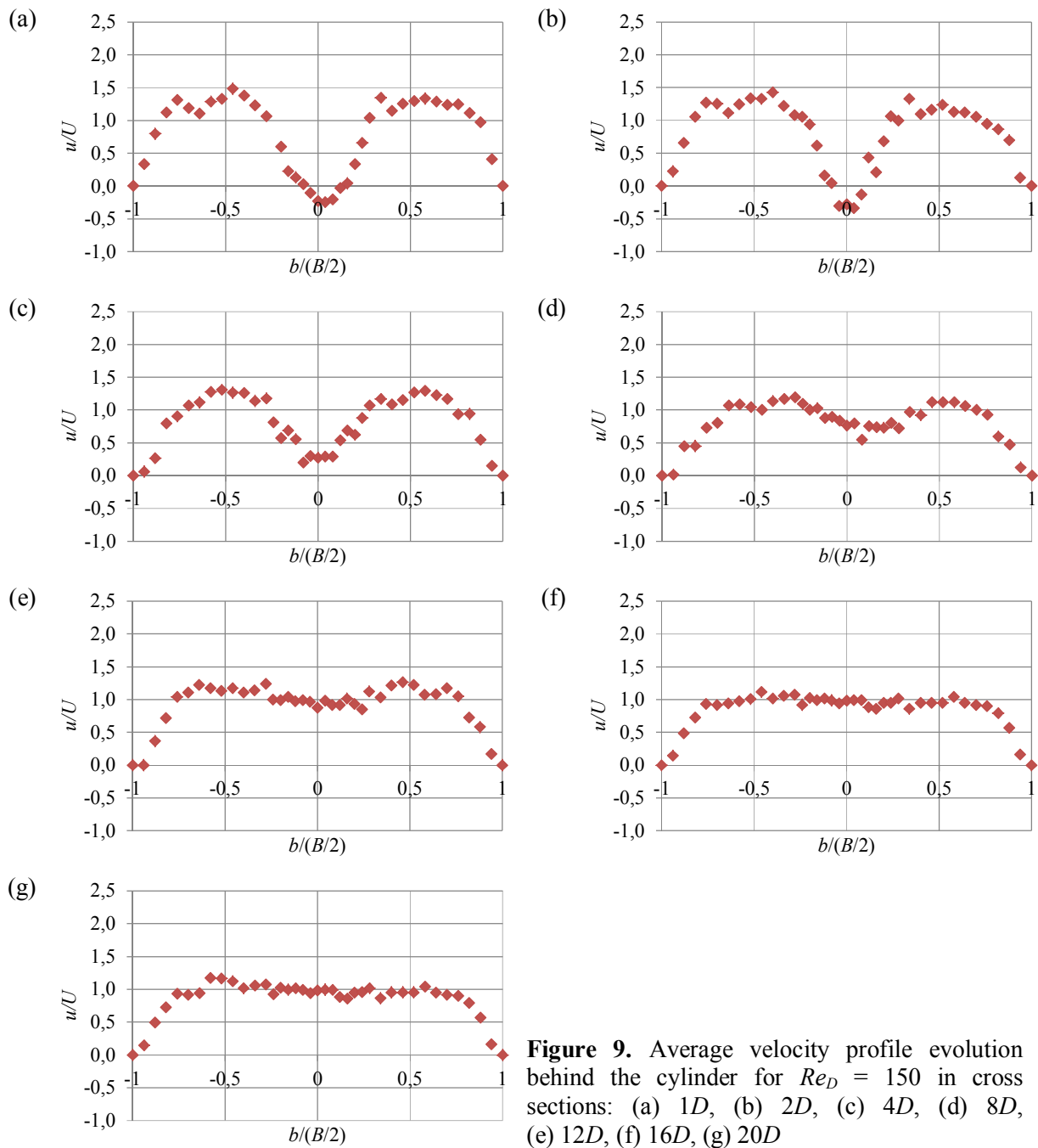


Figure 9. Average velocity profile evolution behind the cylinder for $Re_D = 150$ in cross sections: (a) $1D$, (b) $2D$, (c) $4D$, (d) $8D$, (e) $12D$, (f) $16D$, (g) $20D$

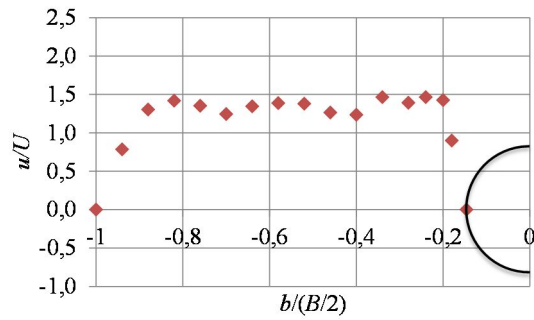


Figure 10. Average velocity distribution in the cross section of the cylinder axis for $Re_D = 250$

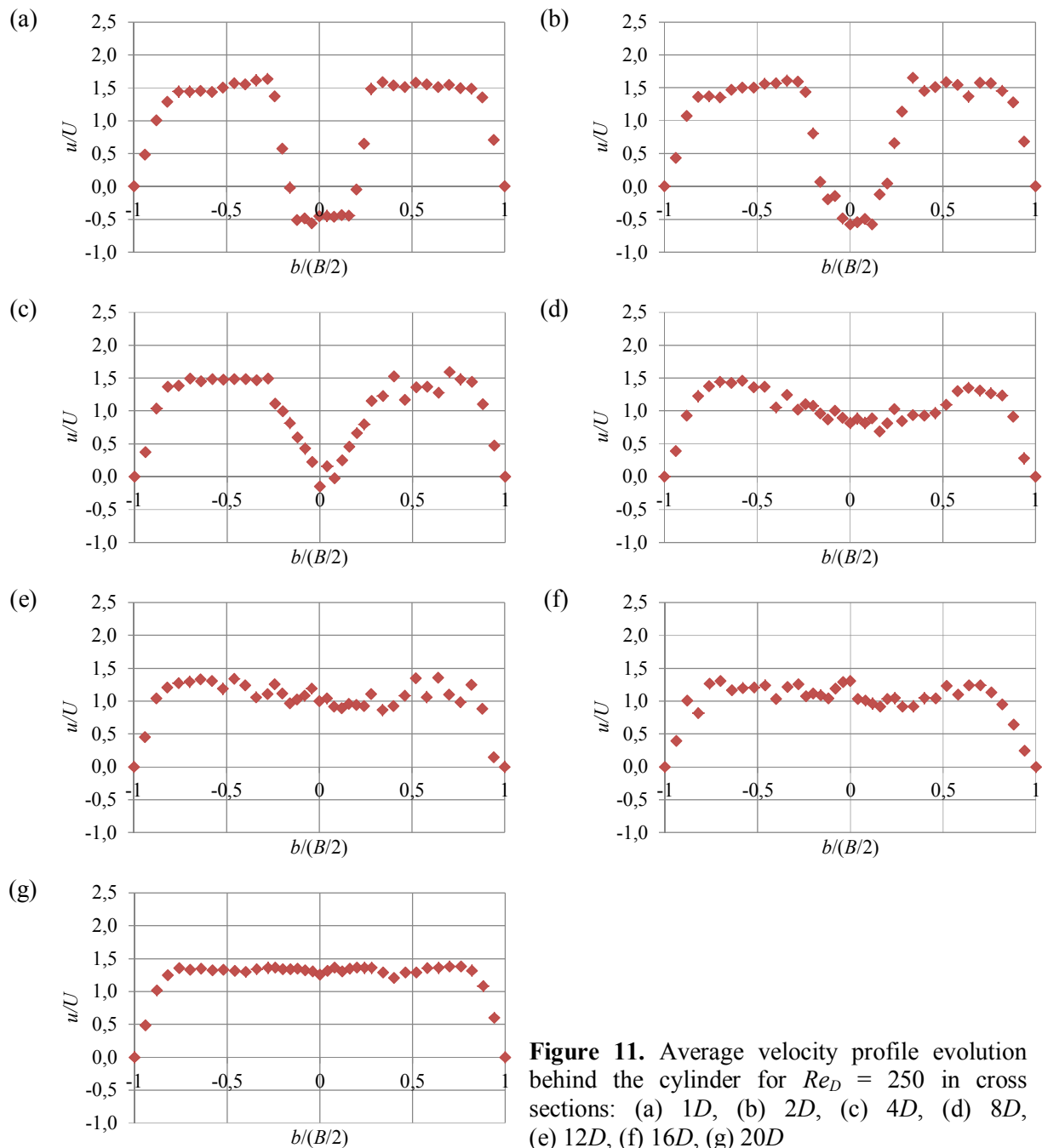


Figure 11. Average velocity profile evolution behind the cylinder for $Re_D = 250$ in cross sections: (a) $1D$, (b) $2D$, (c) $4D$, (d) $8D$, (e) $12D$, (f) $16D$, (g) $20D$

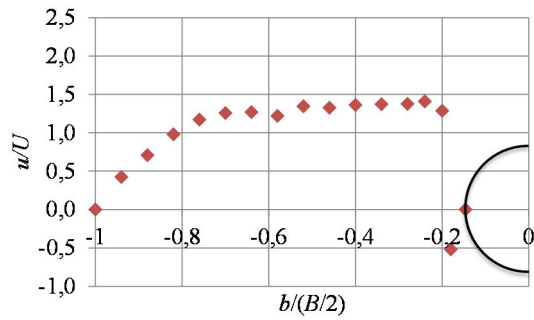


Figure 12. Average velocity distribution in the cross section of the cylinder axis for $Re_D = 350$

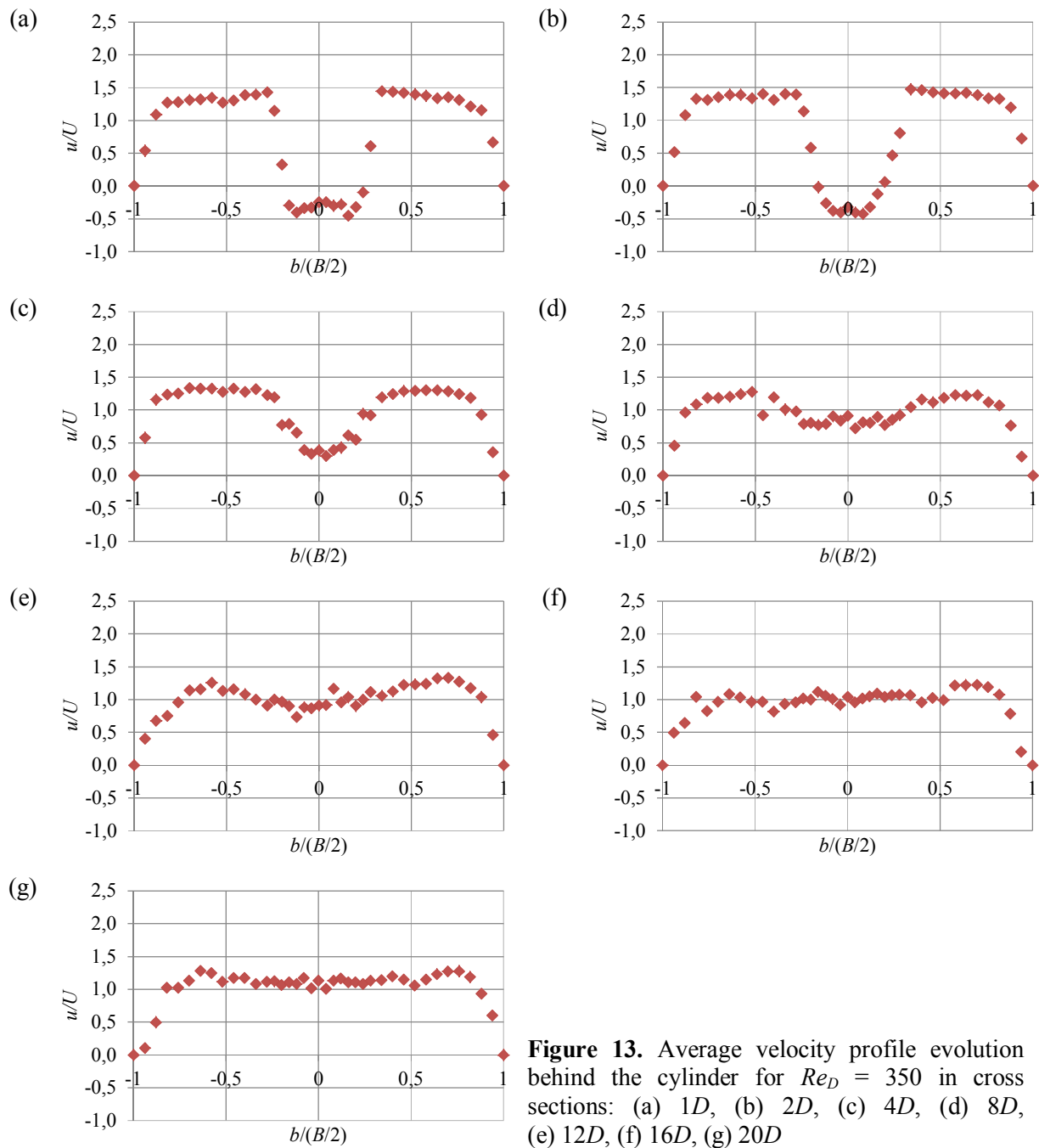


Figure 13. Average velocity profile evolution behind the cylinder for $Re_D = 350$ in cross sections: (a) $1D$, (b) $2D$, (c) $4D$, (d) $8D$, (e) $12D$, (f) $16D$, (g) $20D$

Changing the depth of water in a tunnel changes the nature of the flow (Figure 14 (b)). Although the Re_D does not change, the Re_{h_w} ($Re_{h_w} = U \cdot h_w / \nu$) decreases twice (Table 2). For $h_w = 30$ mm a part of the dye spreads along the tunnel bottom, a part of it is however pulled upwards. At a height of approximately 1/4 of the water depth the dye marker is again taken away and dissipated by the main flow. For $Re_D = 40$ no vortex structure is observed in the wake of the cylinder regardless of the water depth.

For $Re_D = 100$ and $h_w = 65$ mm (Figure 15 (a)) it can be easily seen that the thread of the dye marker is displaced from the bottom surface of the tunnel in the direction of the water level. Pulling out the thread of dye from the bottom of the tunnel may be caused by negative pressure, which is the result of an increase in flow velocity in the area of the free water surface. At the height of approximately 1/2 of the water depth, the dye is rolled up in the direction of the cylinder wall, then dye marker rotates in the direction of cylinder and flows down along the back side of the cylinder. A clear vortex structure increasing with time can be observed. The entire phenomenon takes place only in the lower half of the filling height of the water tunnel.

For $h_w = 30$ mm and the same Re_D (Figure 15 (b)) the thread of dye taken away from the boundary layer and placed in the direction of the water level is rolled up in the direction of cylinder and creates a vortex structure. Initially it is seen only in the lower half of the tunnel, but with time it increases in volume, expands up to the free water surface and finally is extended between the bottom and the free surface. Then the vortex structure "sticks" to the back side of the cylinder.

$Re_D = 150$ and $h_w = 65$ mm (Figure 16 (a)), the dye marker is rapidly pulled off from the bottom of the tunnel in the direction of the free surface. Then the dye starts to vibrate violently showing the disorder. Due to the fact that the velocity of the flow is high, at the height of approximately 3/4 of the water depth, the dye marker is taken away and dissipated by the main stream instead of being rolled up towards the cylinder wall.

After lowering the height of the tunnel to $h_w = 30$ mm (Figure 16 (b)) a gentle thread of dye taken from the boundary layer is observed. It is rolled up in the direction of cylinder wall just under the water level and yields a clear vortex structure. The dye marker "sticks" to the cylinder wall in time, crawling on it and directing to the bottom of the tunnel. Just before the bottom the dye marker is picked up again. The observed vortex structure occupies almost the entire space between the bottom and the water surface.

For both analysed water depths for $Re_D = 250$ a clear vortex structure in the cylinder wake, rotating in the direction of cylinder wall was observed to be formed. In the case of $h_w = 65$ mm (Figure 17 (a)), this structure reaches a height of about 2/3 of the water depth. It should be noted that a considerable amount of dye is placed from the bottom of the tunnel to the interior of the vortex structure. The dye does not spread along the bottom of the tunnel in the direction of the main flow, it is accumulated just behind the obstacle. In the case of $h_w = 30$ mm (Figure 17 (b)) the vortex structure occupies the entire space between the bottom of the tunnel and the water level. It seems to be slightly flattened by the free surface. The dye marker spreads along the tunnel bottom behind the cylinder at a much greater distance than it was for $h_w = 65$ mm.

The increase in the Reynolds number to $Re_D = 350$ causes that regardless of the water depth in the tunnel, a vortex structure is no longer observed in the wake of the bridge pillar model. For $h_w = 65$ mm (Figure 18 (a)), the dye is placed up and dispersed by the main stream of water before it reaches the water level. Due to the very intensive transport upwards, it practically does not spread in the area of the boundary layer. For $h_w = 30$ mm (Figure 18 (b)) the thread of the dye marker reaches the free surface but is immediately taken away by the main flow. A clear vortex structure rotating in the direction of cylinder is not observed.

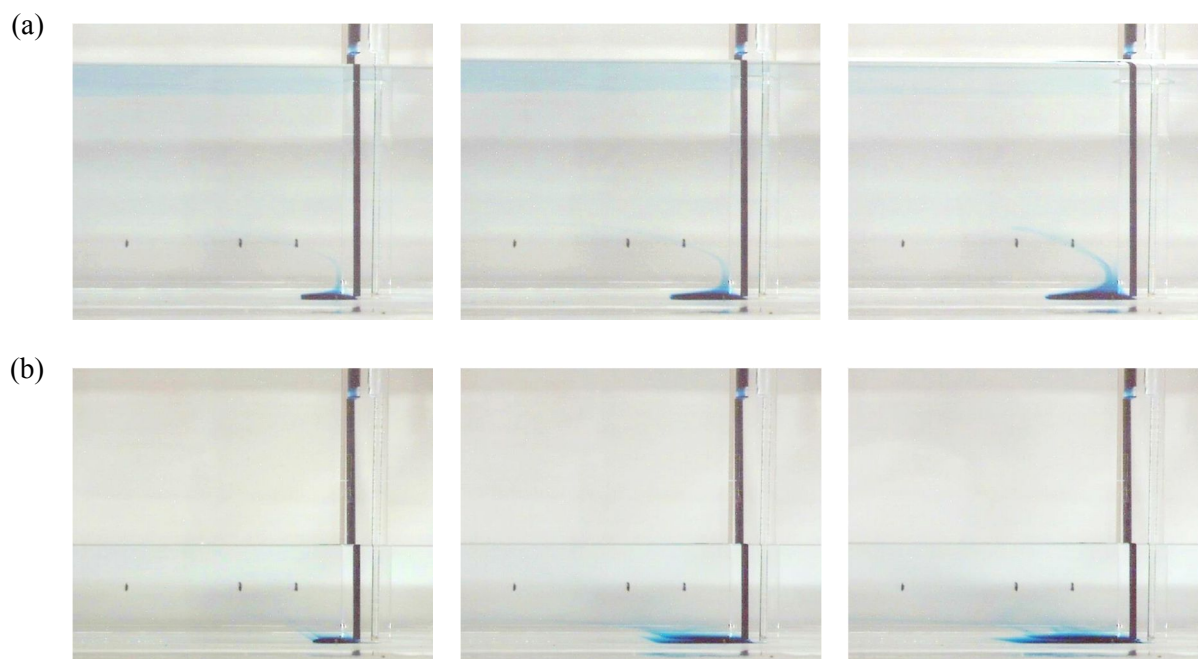


Figure 14. Exemplary images of flow behind the bridge pillar model for $Re_D = 40$, side view: (a) $h_w = 65$ mm, $h_w/D = 4,44$, (b) $h_w = 30$ mm, $h_w/D = 2,05$

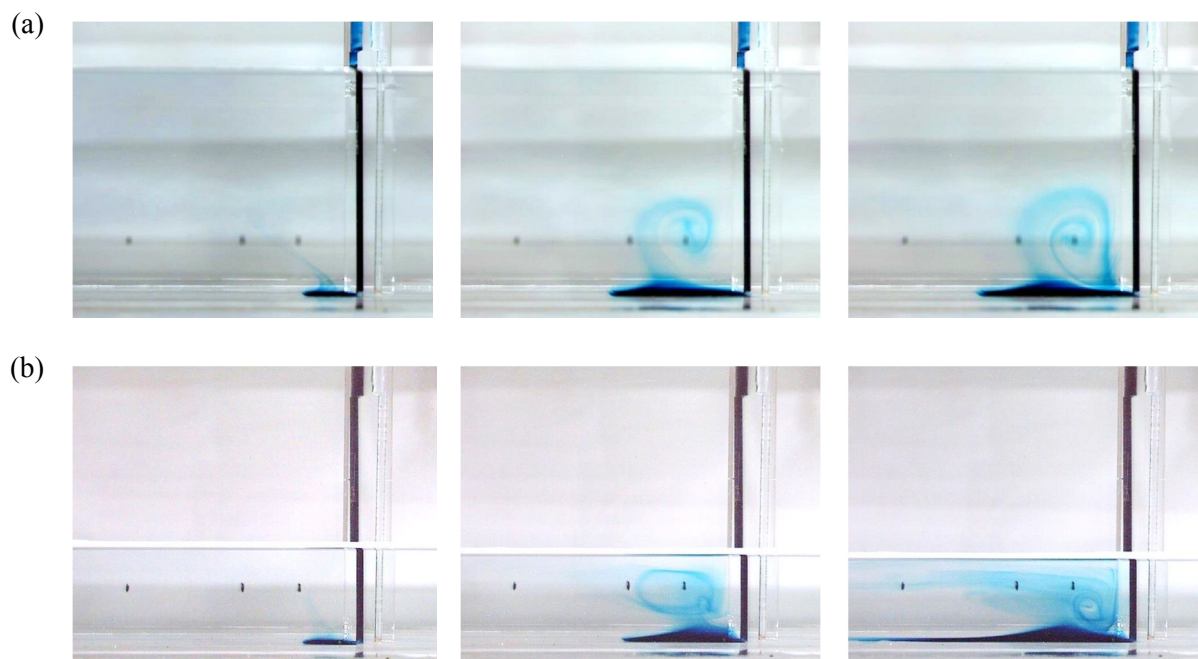


Figure 15. Exemplary images of flow behind the bridge pillar model for $Re_D = 100$, side view: (a) $h_w = 65$ mm, $h_w/D = 4,44$, (b) $h_w = 30$ mm, $h_w/D = 2,05$

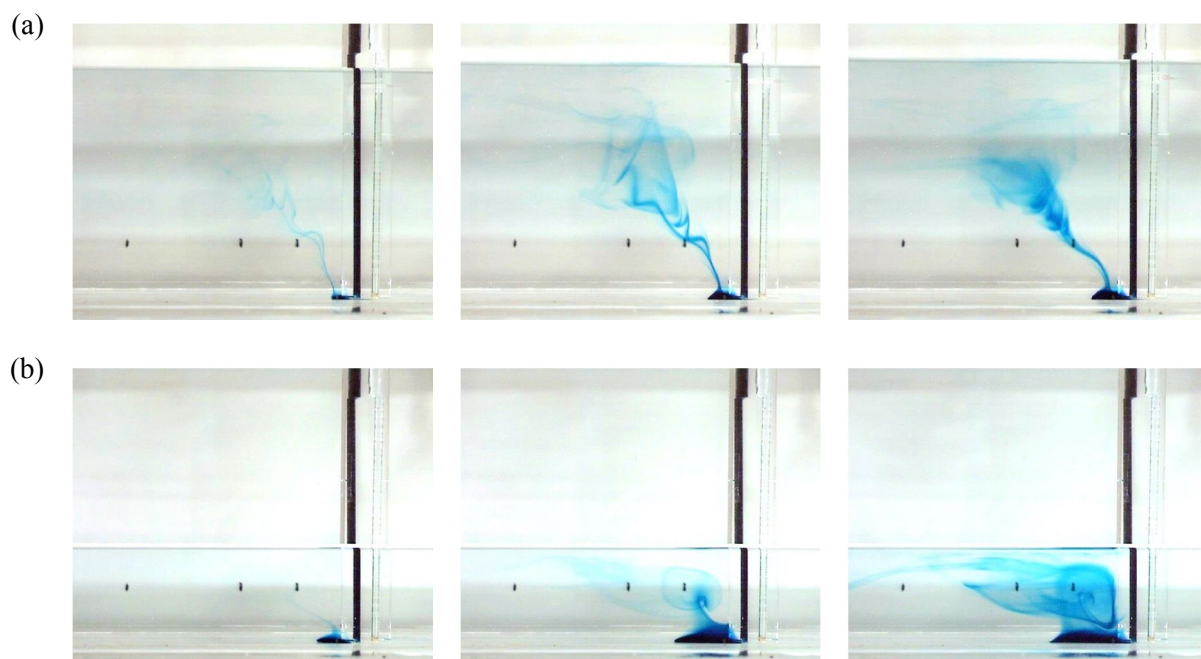


Figure 16. Exemplary images of flow behind the bridge pillar model for $Re_D = 150$, side view: (a) $h_w = 65$ mm, $h_w/D = 4,44$, (b) $h_w = 30$ mm, $h_w/D = 2,05$

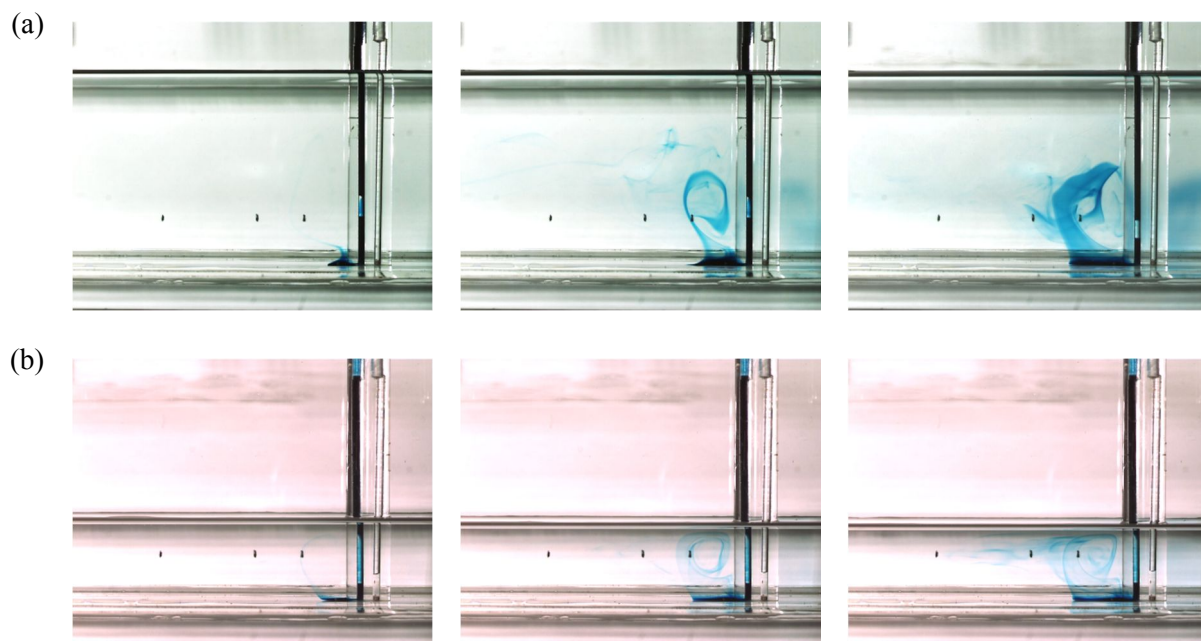


Figure 17. Exemplary images of flow behind the bridge pillar model for $Re_D = 250$, side view: (a) $h_w = 65$ mm, $h_w/D = 4,44$, (b) $h_w = 30$ mm, $h_w/D = 2,05$

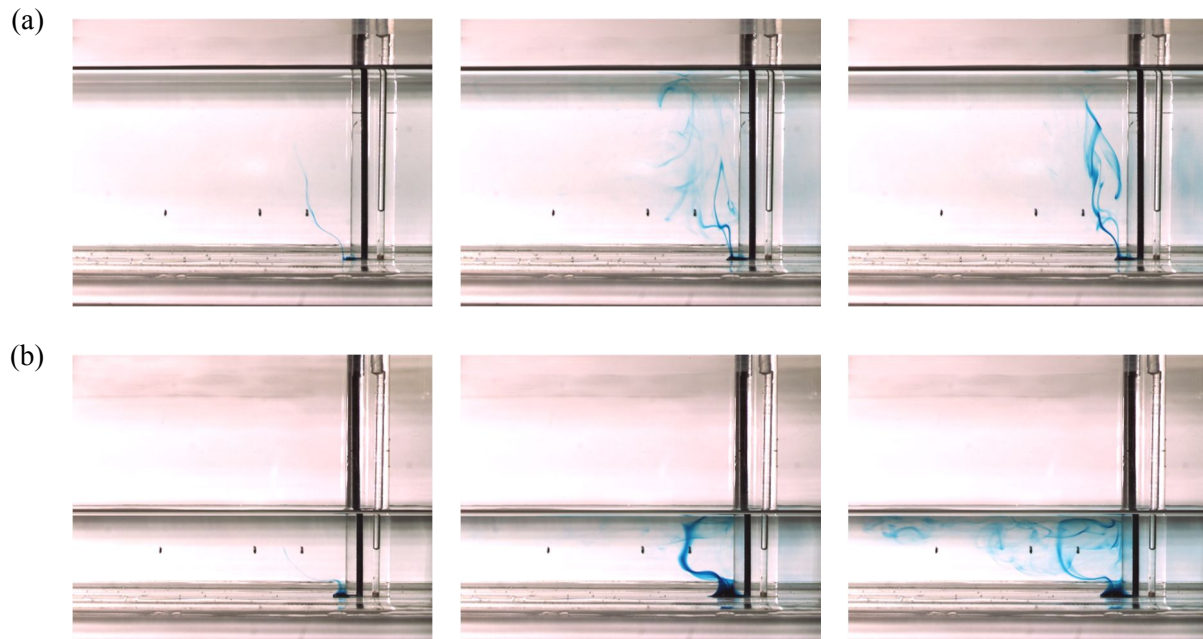


Figure 18. Exemplary images of flow behind the bridge pillar model for $Re_D = 350$, side view: (a) $h_w = 65$ mm, $h_w/D = 4.44$, (b) $h_w = 30$ mm, $h_w/D = 2.05$

5. Summary

Quantitative and qualitative researches of flow around a bridge pillar model (cylinder) for the Reynolds number Re_D ($Re_D = U \cdot D / \nu$) were conducted. All researches were carried out for five values of the Reynolds number $Re_D = 40, 100, 150, 250$ and 300 , therefore laminar flow, laminar–turbulent transition as well as turbulent flow occurred in test section.

Measurements of local average velocity (average in time) using Laser Doppler Anemometry were conducted in order to determine the structure of flow in the area of the bridge pillar model impact. All the anemometric measurement were carried out for constant water depth in a tunnel $h_w = 65$ mm.

Deformation of velocity profiles were observed for each examined Re_D . These deformation was decreasing with the distance from the model and in cross-section $16D$ all profiles were already stable. Recirculation zone behind such an obstacle was observed for each Re_D . For $Re_D = 40$ (the smallest examined Re_D) this recirculation zone a) $\alpha_0 = \pi/6$ ne was reaching the $1D$ cross-section, for $Re_D = 100$ and $150 - 2D$ cross-section, for $Re_D = 250$ and 300 it reaches further distance ($4D$) and is much wider than it was for smaller values of Re_D .

Vortex formation from a vertical cylinder in shallow water was investigated using visualisation by dye marker. Visualization researches were carried out also for five values of the Reynolds number Re_D , but in contrast to anemometric measurements, they were extended to various water depth in the tunnel. Two visualisations were made for each Reynolds number as a consequent. In the first case the water depth was $h_w = 65$ mm, then it was reduced to $h_w = 30$ mm. The purpose of reducing the tunnel filling is to demonstrate the difference in the phenomena occurring in the flow around the cylinder without changing the Re_D , that is, assuming the diameter of the cylinder as a characteristic quantity.

A distinguishing feature of the shallow water wakes is the three-dimensional roll-up of the dye marker between the bottom and the free surface which yields a spiral vortex structure that is possible to be observed when too large disturbances does not occur in a flow. It was observed that the dyed fluid particles spread along the bottom surface of test section are forced to climb up in form of the narrow thread of vorticity. This phenomenon was called as the eruption of the boundary layer.

The mechanism of the dye marker displacing from the tunnel bottom to the main flow remains the same independently of the Reynolds number. However size, shape of the vortex structure and intensity of the dye marker relocation from the area near the bottom to the main flow do vary.

References

- [1] Seal C V and Smith C R 1999 Visualization of a mechanism for three-dimensional interaction and near-wall eruption *J. Fluid Mech.* **394** 193
- [2] Chen D and Jirka G H 1995 Experimental study of plane turbulent wakes in a shallow water layer *Fluid Dyn. Res.* **16** 11
- [3] Akilli H and Rockwell D 2000 Vortex formation from a cylinder in shallow water *Phys. Fluids* **14** 2957
- [4] CHEN D and JIRKA G H 1997 Absolute and convective instabilities of plane turbulent wakes in a shallow water layer *J. Fluid Mech.* **338** 157
- [5] FU H and ROCKWELL D 2005 Shallow flow past a cylinder: control of the near wake *J. Fluid Mech.* **539** 1
- [6] KAHRAMAN A, SAHIN B and ROCKWELL D 2002 Control of vortex formation from a vertical cylinder in shallow water: Effect of localized roughness elements *Exp. Fluids*. **33** 54
- [7] KUDELA H and MALECHA Z M 2006 Badanie zjawiska erupcji warstwy przyściennej metodą cząstek wirowych *Inż. Chem. Proc.* **27** 833
- [8] KUDELA H and MALECHA Z M 2007 Investigation of unsteady vorticity layer eruption induced by vortex patch using vortex particles method *JTAM* **45** 785
- [9] KUDELA H and MALECHA Z M 2009 Eruption of a boundary layer induced by a 2D vortex patch *Fluid Dyn. Res.* **41**
- [10] PN-EN 1205:25
- [11] Sumer B M and Fredsoe J 1999 *Hydrodynamics around cylindrical structures* (Singapore: World Scientific Publishing Co. Pte. Ltd.)
- [12] ELSNER J and DROBNIAK S 1995 *Metrologia turbulencji przepływów* (Wrocław, Warszawa, Kraków: Ossolineum)
- [13] *FlowLite Installation & User's guide* 1995 (Dantec Measurement Technology A/S)
- [14] GOLDSTEIN R 1983 *Fluid mechanics measurements* (Washington, New York, London: Hemisphere Publishing Corporation)